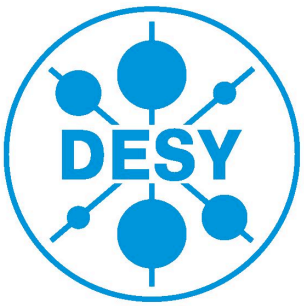

Ptychographical measurements of biological specimen

Karolina Stachnik

AGH University of Science and Technology, Poland

Supervisor: Alke Meents

September 6, 2012

Abstract

This report summarizes my work as a DESY summer student in Hamburg. It sheds a light on a promising coherent x-ray diffractive imaging (CXDI) method called ptychography. The theoretical background of CXDI is discussed to emphasize the crucial features and parameters. Further on, the ptychographical CDI is introduced with outpointed differences to the conventional CDI. The problem of the optimum relative overlap is presented. The operation of the extended ptychographical iterative engine is explained and the experimental part, carried out at P11 beamline of PETRA III synchrotron, is described. As a proof of a considerable potential of ptychography, the example applications of this method are analyzed.

Contents

1 Introduction

The purpose of this report is to present and evaluate my work as a DESY summer student in Hamburg this summer. I was participating in the photon science part activities and was assigned to Alke Meents' research group who was also my supervisor. My project was focused on investigating a new technique in the field of coherent (lensless) x-ray microscopy called ptychography. This report shall give an overview of this method and refer to all the aspects of my contribution to this project.

2 Theory

2.1 Coherent Diffractive Imaging

Coherent X-ray Diffractive Imaging (CXDI) original experimental realization is very similar to conventional crystallography. To illuminate the specimen a plane wave is used and a far field diffraction pattern is collected on a two-dimensional detector. Unlike in crystallography, however, the specimen is not crystalline. As a result, the diffraction pattern is not a collection of isolated Bragg peaks, but a continuous intensity distribution, sampled at the location of the detector pixels. As only the wave field intensity can be measured in the detector plane, a recovery of the phase information is necessary to reconstruct an image of the object in real space.
In 1999 the first experimental demonstration of coherent x-ray diffractive imaging was achieved in the (soft) x-ray energy range, again enabled by the high degree of coherence provided by a synchrotron source. Largely driven by the potential to overcome technical restrictions in the fabrication of x-ray lenses, the technique has been applied successfully by now to single freeze-dried and frozen-hydrated cells, with a potential to exceed the resolution of conventional x-ray microscopy which is limited by the lenses. As a result of the Shannon theorem, for plane wave illumination sufficient sampling of the diffraction pattern and therefore reconstruction is only possible, if the object has a finite extension in real space. As a consequence, the classical scheme of CXDI does not allow for the application to extended specimens, such as multicellular arrangements exceeding the cross-section of the illumination. This limitation has motivated the development of alternatives which allow for the combination of scanning microscopy with diffraction microscopy. [1] One of them is discussed in following chapters.

In Figure 2.1 the schematic of Fresnel coherent diffractive imaging experiment is presented. The sample is illuminated with a nominally coherent beam of X-rays and the

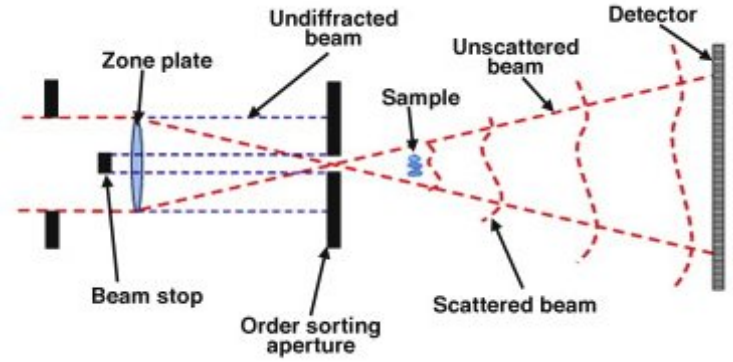

Figure 2.1: The Fresnel coherent x-ray diffractive imaging experiment scheme. [2]

resulting diffraction pattern is captured on a suitable detector placed downstream of the sample. The first pinhole is used to select a coherent patch of the beam. A beam stop (central stop) is introduced to prevent the direct beam from the synchrotron damaging the detector. A zone plate is here used to create a diverging beam to be incident on the sample. Assembly of an order sorting aperture (OSA) allows to remove other diffracting orders from the zone plate and also, in conjunction with a beam stop upstream of the OSA, to prevent the undiffracted beam (0th zone plate order, the edges of which are shown as blue dotted lines) from reaching the detector. [2] None of sofisticated x-ray lenses is applied to CXDI setup which makes the final images free from aberration and resolution limited ultimately by the illumination wavelength.

What should be exphasized is a fundamental drawback of diffraction-based imaging: the phase problem. The recorded real-valued data contain only aplitude information and the equally important knowledge of the phase values are lost. For the different fields of diffraction and microscopy various solutions have been suggested to retrieve the phase information. [4] The certain number of iterative phase retrieval methods involves algorithms which lead to unambiguous phase regain by the alternations between real and Fourier space with certain boudary constraints.

2.2 Ptychography

Ptychographical coherent diffractive imaging (PCDI), a combination of iterative phase retrieval with scanning microscopy, was the first demonstrated extension of the original CXDI scheme to overcome its field of view limitation. It is also called ptychography,

which origins from the Greek word "$\pi\tau\nu\xi$" meaning "fold". Here a localized illumination, e.g. provided by an unfocused synchrotron beam confined by a small pinhole (of a micron-range diameter), is used to probe an extended specimen at varying in lateral positions. [1]

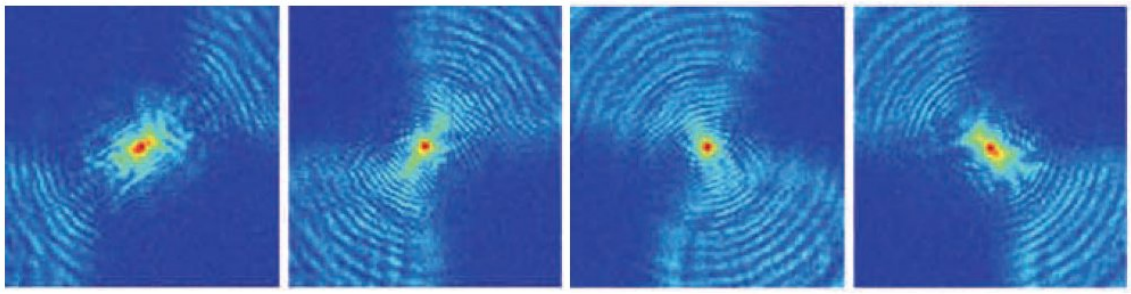

Figure 2.2: Four (out of 225) coherent x-ray diffraction patterns (displayed on logarithmic colourscale) of gold nanostructures. [3]

An ensemble of a number of Fraunhofer diffraction patterns is collected (Figure 2.2). Each of these patterns originates from a different but overlapping region of the specimen, which, as already mentioned, is moved laterally across the illuminating beam (Figure 2.3a). The solution strategy is to iteratively reconstruct and refine a single projection of the sample, which is consistent with all the recorded diffraction patterns. [3] Result of such a reconstruction is shown in Figure 2.3b.
What is quite important, is that with the term *overlap* a linear distance offset is meant, not area overlap. For two circles of radius r and the centre-to-centre distance $a \in [0, 2r]$ one can define the absolute overlap o_{abs}

$$o_{abs} = 2r - a$$

Normalized by the diameter of the circles the relative overlap o is given by

$$o = 1 - \frac{a}{2r} \tag{2.1}$$

In [4] one can find a valuable discussion of determining the optimum overlap of the different illumination positions. The simulated object shown in Figure 2.4 was scanned with 5x5 positions of different overlaps.
The result is shown in Figure 2.5. In Figure 2.5(a) the relative overlap of the positions (see Eq. (2.1)) is only 10%. The reconstructed image hardly resembles the original one. When the relative overlap is increased to 60%, the retrieved image cannot be distinguished by eye from the original one (Figure 2.4(b)). With 100% relative overlap

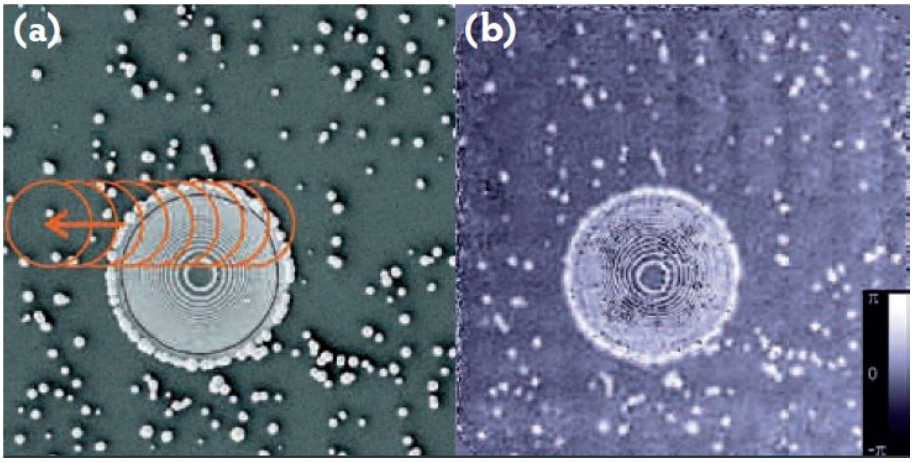

Figure 2.3: (a) Scanning electron micrograph of the test sample with gold nanostructures. The circles indicate positions for which diffraction patterns were recorded.
(b) Phase of the reconstructed complex-valued exit wave of the specimen (linear colourscale). The images represent a filed of view of 52x52 μm^2. [3]

the reconstruction algorithm degenerates to a conventional iterative phase retrieval, resulting in again poor image quality. [4] Generally, it is advised in ptychographical experiments to keep the illuminated areas of the specimen overlap by around 70%.

2.3 Ptychographical Iterative Engine

Iterative phase retrieval is one method of recovering a complex-valued reconstruction of a sample from measurement of its diffraction pattern. This is achieved by iteratively enforcing a set of constraints corresponding to the measurements taken and a priori knowledge of the system. [6]
The crucial step for the application to non-crystalline samples was then the implementation of concepts from iterative phase retrieval for the analysis of a ptychographical dataset into an algorithm that was named the Ptychographical Iterative Engine (PIE). [1] However, a considerable drawback of the PIE is that it requires accurate model of the localised wavefront which illuminates the target object. With this requirement the quality of the object function may never be better than the quality of the guessed illumination. Therefore, an extension of the original PIE has been developed to introduce the simulaneous reconstruction of both the object function and the complex illumination (the probe).
In this scope, I shall refer to this extended Ptychographical Iterative Engine (ePIE) as a more efficient solution to the ptychographical problem bringing a major improvement

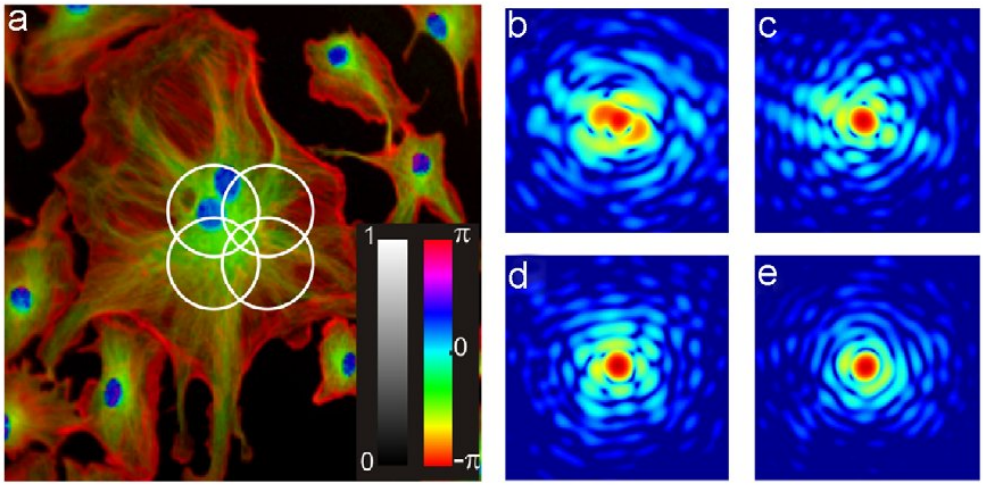

Figure 2.4: Sample image and some diffraction patterns for the positions indicated in the image (a). [4]

in reconstruction process. For more detailed description, see [6].
The operation of the ePIE is depicted in Figure 2.6. It is assumed that the interaction between the sample and the probe can be modelled by a complex multiplication. The wavefront exiting the sample is termed the exit wave and the further assumption is that its propagation to the plane of the detector can be momdelled by a Fourier transform (high degree of coherence required from the probe at the plane of the sample). Therefore, the intensity of the wavefront incident at the detector is given by the formula

$$I_j(\boldsymbol{u}) = |\mathcal{F}[O(\boldsymbol{r})P(\boldsymbol{r} - \boldsymbol{R_j})]|^2 \tag{2.2}$$

where $\boldsymbol{r}$ and $\boldsymbol{u}$ are real-space and reciprocal-space coordinate vectors and $O(\boldsymbol{r})$ and $P(\boldsymbol{r})$ denote the object and the probe wavefronts, respectively. The vector $\boldsymbol{R_j}$ encodes the relative shift which is introduced between the object and probe before the intensity of the jth diffraction pattern is recorded.

Initial guesses ($j = 0$), $O_0(\boldsymbol{r})$ and $P_0(\boldsymbol{r})$, are required to begin the algorithm. Generally, the initial object guess is taken as free-space and the initial probe wavefront is taken as a support function roughly the size of the intense region of the probe wavefront. The diffraction patterns are addressed in a random sequence *s(j)*. Beginning with pattern *s(0)*, a guess at the exit wave is formed by multiplying the current object guess by the

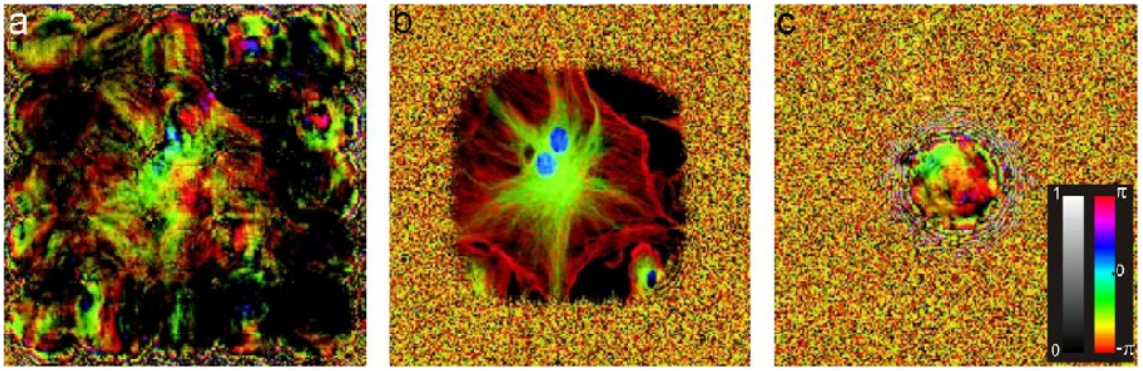

Figure 2.5: Reconstruction for different relative overlaps.
The relative overlap of the object position:
(a) 10%, (b) 60%, (c) 100%. [4]

appropriately shifted probe guess, which gives

$$\psi_j(\boldsymbol{r}) = O_j(\boldsymbol{r})P_j(\boldsymbol{r} - \boldsymbol{R_{s(j)}}) \tag{2.3}$$

The next step is substituting the positive square-root of the *s(j)*th diffraction pattern recording for the modulus of the Fourier transform of this exit wave, so that

$$\Psi_j(\boldsymbol{u}) = \sqrt{I_{s(j)}(\boldsymbol{u})}\frac{\mathcal{F}[\psi_j(\boldsymbol{r})]}{|\mathcal{F}[\psi_j(\boldsymbol{r})]|} \tag{2.4}$$

An updated exit wave is then calculated with a use of an inverse Fourier transform

$$\psi'_j(\boldsymbol{r}) = \mathcal{F}^{-1}[\Psi_j(\boldsymbol{u})] \tag{2.5}$$

Finally, updated object and probe guesses are extracted from this result using two update functions. Eq. (2.6), update function 1, updates the current object guess and is given by

$$O_{j+1}(\boldsymbol{r}) = O_j(\boldsymbol{r}) + \alpha\frac{P_j^*(\boldsymbol{r} - \boldsymbol{R_{s(j)}})}{\max(|P_j(\boldsymbol{r} - \boldsymbol{R_{s(j)}})|^2)}(\psi'_j(\boldsymbol{r}) - \psi_j(\boldsymbol{r})) \tag{2.6}$$

Whereas the following equation describe the update of the probe (update function 2)

$$P_{j+1}(\boldsymbol{r}) = P_j(\boldsymbol{r}) + \beta\frac{O_j^*(\boldsymbol{r} + \boldsymbol{R_{s(j)}})}{\max(|O_j(\boldsymbol{r} + \boldsymbol{R_{s(j)}})|^2)}(\psi'_j(\boldsymbol{r}) - \psi_j(\boldsymbol{r})) \tag{2.7}$$

where $\alpha, \beta \in [0, 1]$ are constants adjusted to alter the step-size of the update.

The process presented above is continued with diffraction pattern $s(1), s(2), \ldots, s(J)$ until each of the J diffraction patterns have been used to update the object and probe guesses. At this point a single ePIE iteration is completed. Depending on a chosen implementation, 20 to 30 iterations are needed to obtain final reconstruction image.

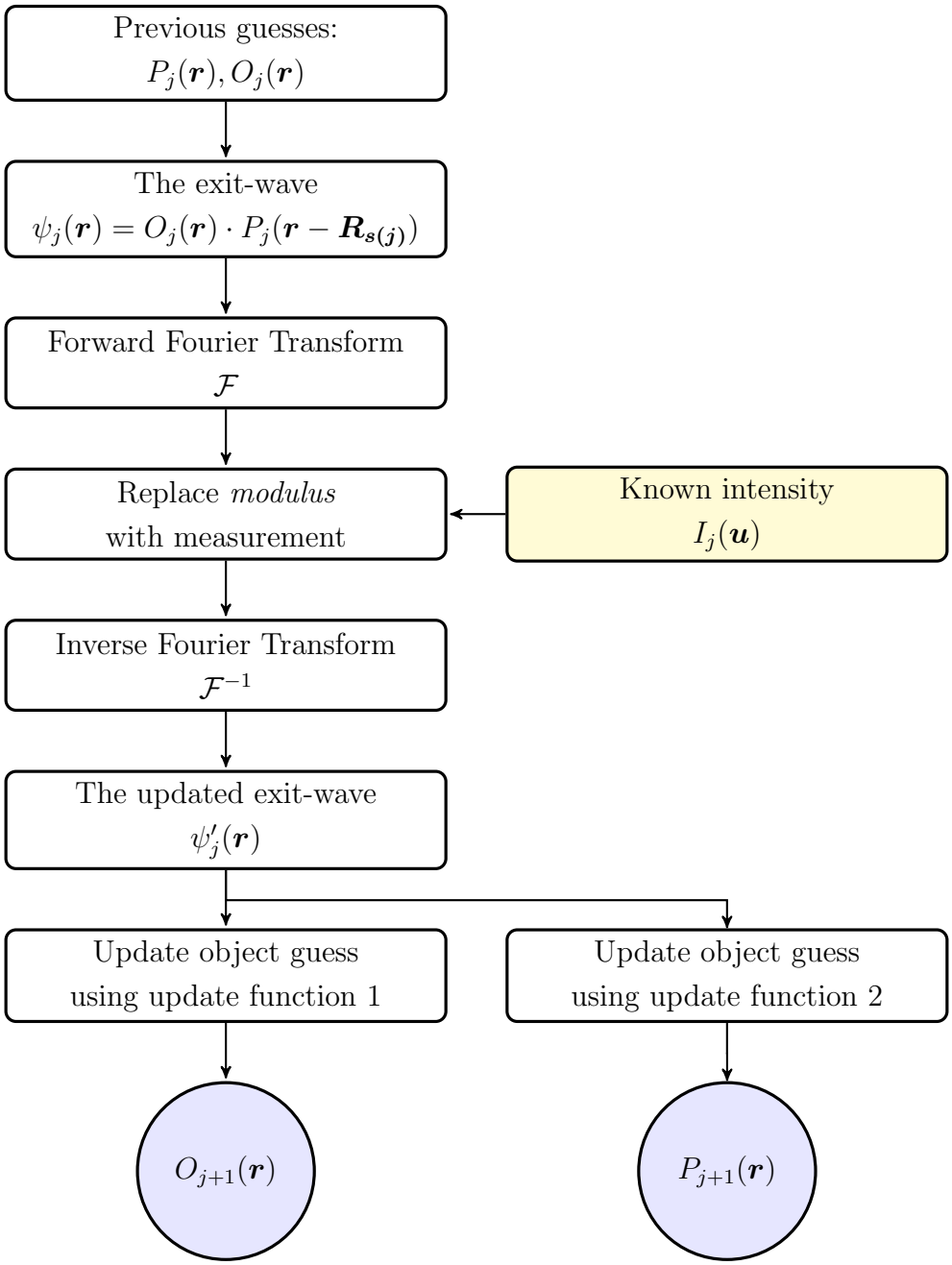

Figure 2.6: Flowchart of the ePIE method.

3 Measurement

3.1 Experimental setup

The crucial part of my project was participation in experimental setup preparation. The experiment was carried out at beamline P11 of PETRA III synchrotron light source. The scheme of the ptychography experiment is shown in Figure 3.1.

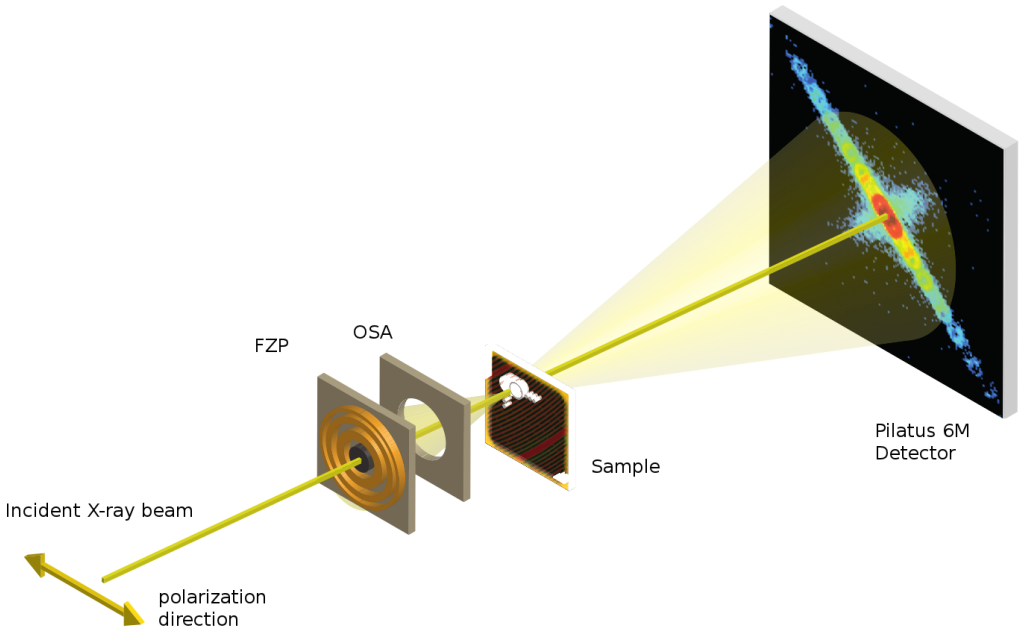

Figure 3.1: Example of experimental setup for ptychography x-ray imaging.

The well-defined and collimated undulator beam of 7.5 keV energy was used as a source of illumination. The probe was formed using (Figure 3.2): beam defining pinhole (BDP) of diameter 150 μm and central stop (CS), mounted next to the Fresnel zone plate (FZP) upstream to the beam, the Fresnel zone plate of focal length 2.3 cm and the order sorting aperture (OSA) of diameter 10 μm. The sample was mounted on a computer-controlled piezomotorized cartesian x/y stage. The Pilatus 6M detector was collecting ptychographical data placed 636 cm from the sample stage downstream to the beam.
To prevent diffracted x-rays from absorption in air on their quite long relative way to the detector, a flight tube was installed between the sample stage and the detector (Figure 3.3). Inside the flight tube vacuum was kept to reduce signal loss. Two kapton windows were mounted on flight tube's ends because of its high x-ray transmittance and insensitivity to radiation damage.

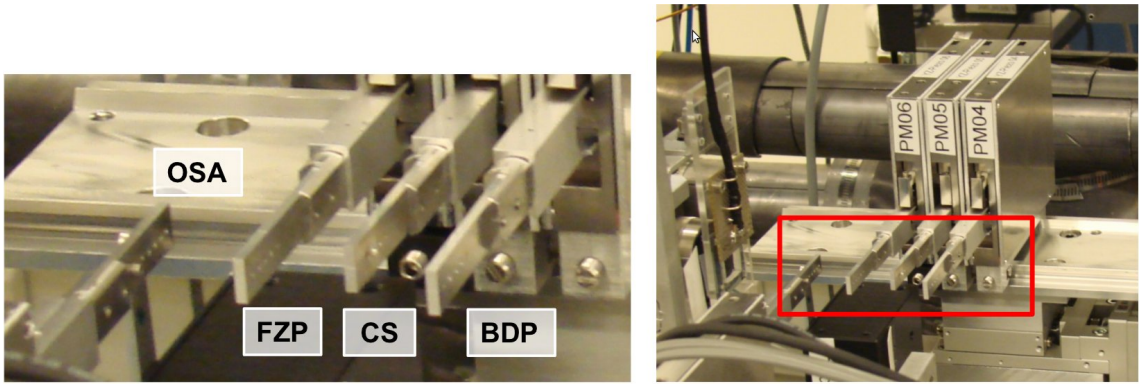

Figure 3.2: Probe defining instruments.

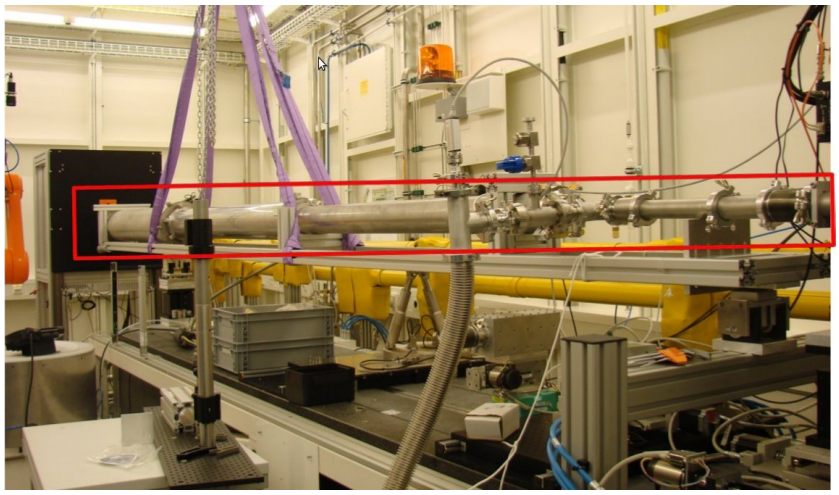

Figure 3.3: P11 beamline ptychography experimental setup - the flight tube (maked in red).

During the beamtime our aim was to apply the setup presented above to ptychographical bio-imaging of the Schistosoma parasite (known commonly as blood-flukes) which is responsible for a highly significant parasitic infection of humans by causing the disease schistosomiasis. However, due to several technical problems which shortened significantly the experimental time, measurements came out to be inconclusive and its analysis is excluded from this report. Yet, more promising is the fact that next attempts for ptychography have been already planned at P11 beamline so, taking into account the significant potential of this beamline, the upcoming future may come with the new complex ptychographical measurements of biological specimen with resolution reaching even 10 nm.

3.2 Applications

Once the ptychographical coherent diffractive imaging proved to be practical and efficient it has been already applied in considerable number of x-ray microscopy experiments. Being recognized also as a high-resolution tomography technique, ptychography provides invaluable information in both the life and materials sciences. Since it was introduced, a significant number of the ptychographical iterative engine implementations has been developed. Let these two examples be a short overview of possible applications of ptychography and its quality.

Figure 3.4 depicts the experiment carried out on lily pollen. Figures 3.4(a) and 3.4(b) show the modulus and phase, respectively, of the ePIE reconstruction of the measured data. They are compared with another implementation of the PIE, refered as the superresolution ptychographical iterative engine (SR-PIE), which is widely discussed in [5]. Figures 3.4(c) and 3.4(d) present in the similar fashion the modulus and phase reconstruction of the SR-PIE.

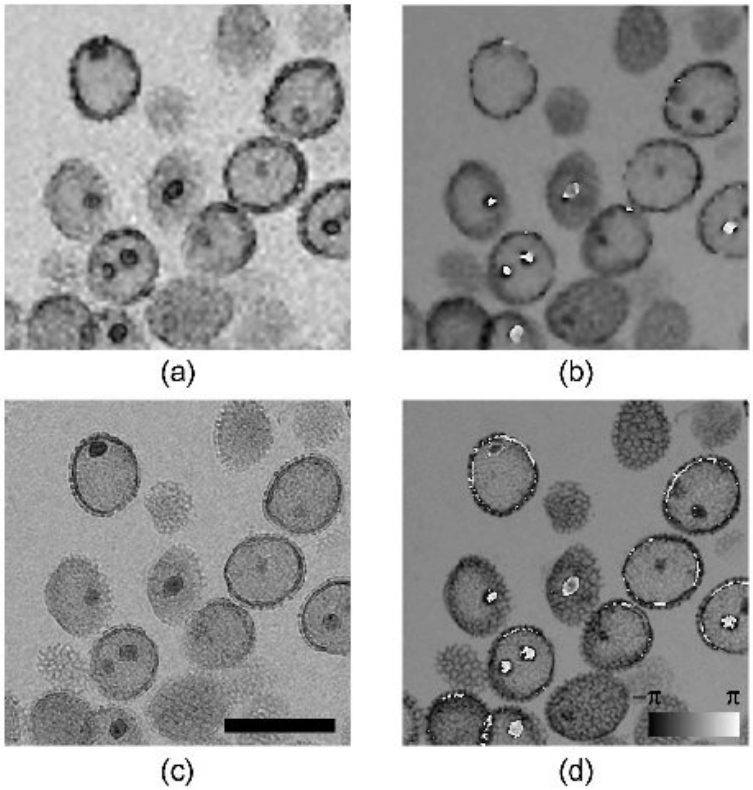

Figure 3.4: Modulus (a) and phase (b) of lily pollen images reconstructed using the ePIE, (c) and (d) superresolved modulus and phase images produced by the SR-PIE. [5]

Another example compares amplitude images reconstruced with the PIE (no probe retrieval) to the parallel ptychographical iterative engine (pPIE), described in [6].

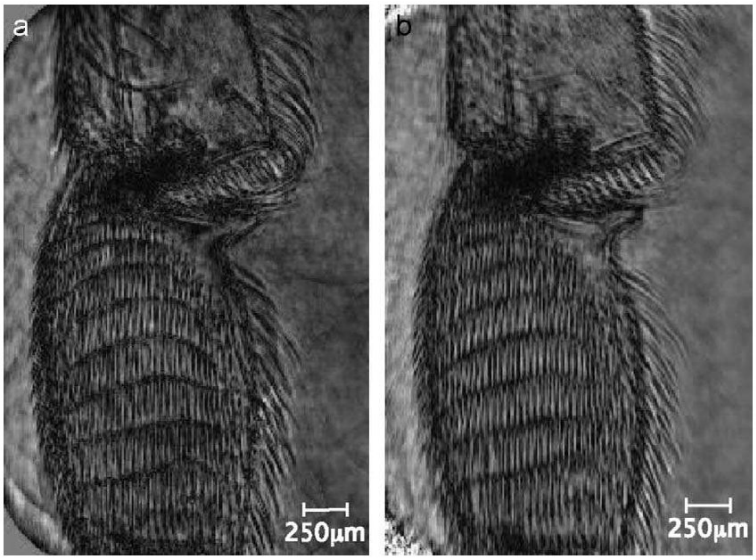

Figure 3.5: The amplitudes of the final reconstructions with (a) the PIE and (C) the pPIE. [6]

4 Conclusions

The ptychographical coherent x-ray diffractive imaging is a powerful and promising method yielding almost diffraction-limited resolution with no use of any lenses or optical components. It was proved in considerable number of applications including nanoscale bio-imaging. According to the simulated data, the optimum relative overlap of a different illuminations is around 70%. So far, a significant number of ptychographical iterative engine implementations has been developed, constantly improving the quality of reconstruced images.

My project allowed me to study the theoretical background of ptychography, work with experimental setup as well as constribute to the ptychographical software developed by Alke Meents' group together with scientists from European XFEL: Klaus Giewekemeyer, Adrian Mancuso and Chun Hong Yoon.

References

[1] A study on new approaches in coherent x-ray microscopy of biological specimens, *K. Giewekemeyer*

[2] Imaging cellular architecture with X-rays, *C. A. Larabell, K. A. Nugent*

[3] Ptychography and lensless X-ray imaging, *M. Dierolf et al.*

[4] Influence of the overlap parameter on the convergence of the ptychographical iterative engine, *Oliver Bunk et al.*

[5] Superresolution imaging via ptychography, *A. M. Maiden, M. J. Humphry, F. Zhang, J. M. Rodenburg*

[6] An improved ptychographical phase retrieval algorithm for diffractive imaging, *A. M. Maiden, J. M. Rodenburg*